TRANSPORTATION RESEARCH BOARD
NATIONAL RESEARCH COUNCIL

IDEA

Innovations Deserving Exploratory Analysis Project

NATIONAL COOPERATIVE HIGHWAY RESEARCH PROGRAM

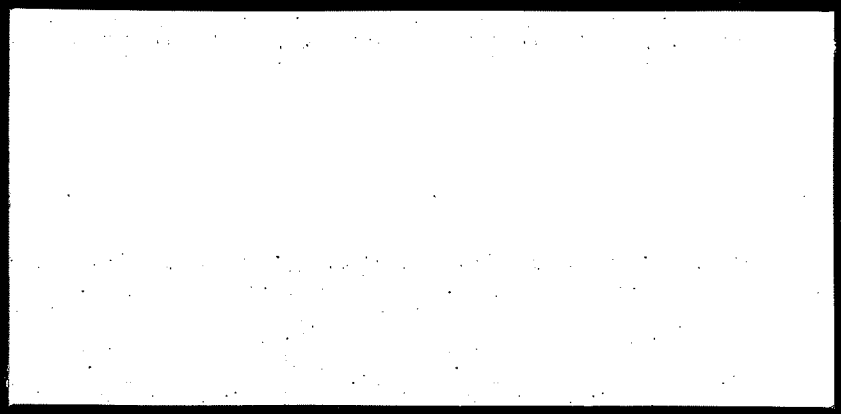

Report of Investigation

IDEA PROGRAM FINAL REPORT

Contract NCHRP – 48

IDEA Program
Transportation Research Board
National Research Council

March 2000

FIELD TRIAL OF SHAPE MEMORY-BASED REHABILITATION SYSTEM

Prepared by:
Ken Ostowari, DPD, Inc., Lansing, Michigan
Parviz Soroushian, Michigan State University

INNOVATIONS DESERVING EXPLORATORY ANALYSIS (IDEA) PROGRAMS
MANAGED BY THE TRANSPORTATION RESEARCH BOARD (TRB)

This NCHRP-IDEA investigation was completed as part of the National Cooperative Highway Research Program (NCHRP). The NCHRP-IDEA program is one of the four IDEA programs managed by the Transportation Research Board (TRB) to foster innovations in highway and intermodal surface transportation systems. The other three IDEA program areas are Transit-IDEA, which focuses on products and results for transit practice, in support of the Transit Cooperative Research Program (TCRP), Safety-IDEA, which focuses on motor carrier safety practice, in support of the Federal Motor Carrier Safety Administration and Federal Railroad Administration, and High Speed Rail-IDEA (HSR), which focuses on products and results for high speed rail practice, in support of the Federal Railroad Administration. The four IDEA program areas are integrated to promote the development and testing of nontraditional and innovative concepts, methods, and technologies for surface transportation systems.

For information on the IDEA Program contact IDEA Program, Transportation Research Board, 500 5th Street, N.W., Washington, D.C. 20001 (phone: 202/334-1461, fax: 202/334-3471, http://www.nationalacademies.org/trb/idea)

CONTENTS

EXECUTIVE SUMMARY

Shape memory alloys can recover deformations induced at lower temperatures upon heating above a transformation temperature. Restraint of this shape recovery tendency can generate large forces. Our approach uses the forces generated during restrained shape recovery to transfer corrective forces to structural systems for accomplishing strengthening and repair tasks. For this purpose, shape memory rods are pre-elongated, anchored onto the structural system, and then subjected to electrical resistance heating to prompt shape recovery and transfer corrective forces to the structure.

Characterization of iron-based shape memory alloys of relatively low cost for application to infrastructure systems was the first task performed in this project. The alloy composition capable of generating relatively high and stable stress levels upon restraint of shape recovery was selected for use in the project. Preliminary laboratory tests verified the ability of pre-elongated rods anchored onto damaged structural systems to restore structural integrity through application of corrective forces. Subsequent damaging effects after installation and initial corrective action of shape memory rods could also be overcome by electrical resistance re-heating of rods.

A reinforced concrete bridge structure with beams lacking sufficient shear strength at longitudinal bar cut-off locations was selected for field demonstration of the technology. The beams in this bridge structure had suffered shear cracking at bar cut-off locations. A design methodology was developed to determine the effects of local post-tensioning with shape memory rods on the shear strength of reinforced concrete beams. The approach was verified through laboratory tests simulating conditions of the selected bridge structure. Subsequently, a detailed design was developed and the approach was implemented under field conditions for the application of local corrective forces to raise the shear strength of a reinforced concrete beam in the selected bridge at bar cut-off location.

Application of corrective (post-tensioning) forces to structural systems using shape memory steel provides an efficient, rapid and convenient approach for repair and strengthening of damaged or deficient structural systems. The relatively large recoverable strains of shape memory alloys help reduce losses of the corrective post-tensioning force. Damaging effects incurred subsequent to installation of shape memory rods can also be overcome by re-heating of the rods. The approach is versatile and suits application to diverse fields of application for corrective effects and for the control of stresses, deflections and instabilities.

1.0 INTRODUCTION AND OBJECTIVES

1.1 INTRODUCTION

Structural deficiencies of bridges, caused by damaging load and environmental effects, faulty design practices or increased traffic loads, represent a major problem of our transportation infrastructure. The shape memory-based rehabilitation system developed and demonstrated in this NCHRP-IDEA project promises to provide a rapid, efficient and low-cost approach with high levels of safety and reliability for the rehabilitation of deficient bridge structures.

Shape memory materials will, after an apparent plastic deformation return to their original shape when heated; constraint of this shape recovery can generate a considerable force. The shape memory effect depends on the occurrence of a specific phase change in the material known as martensitic transformation.[1] At temperatures below the transformation temperature, shape memory alloys are martensitic. Heating above the transformation temperature prompts recovery of the austenite (parent) phase. Martensite and austeniste phases of the same shape memory alloy exhibit distinctly different material properties. Figure 1a schematically shows martensite and austenite stress-strain curves. The austenite phase possesses a memory shape which, irrespective of deformations in the martensite phase, would be recovered upon phase transformation. Figure 1b presents the process of free recovery; this is caused, after an apparent plastic deformation in the martensite phase, by phase transformation through heating. Figure 1c shows the generation of force when martensite (low-temperature) strains cannot be recovered upon heating due to the presence of constraints against strain recovery.

Shape memory alloys based on nickel-titanium (Ni-Ti) have found broad commercial applications.[1] Shape memory alloys of lower cost have also been developed based on iron;[2-6] such low-cost alloys open the prospects for applications of shape memory effect in infrastructure systems.

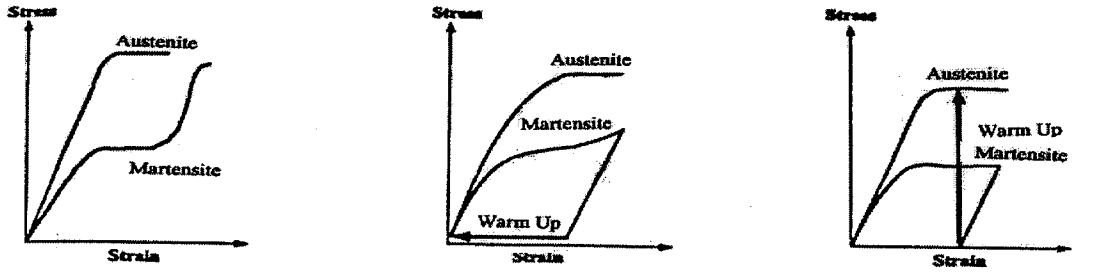

(a) Stress-Strain Curves (b) Free Recovery (c) Constrained Recovery

Figure 1. Shape Memory Behavior.

Our approach relies on the restrained recovery of shape memory alloys to rehabilitate and strengthen existing bridge structures. This approach (see Figure 2) uses shape memory rods which are pre-elongated in the martensite phase and then anchored onto the deficient

structural system; upon (electrical resistance) heating and transformation to austenite phase, constraint of shape recovery causes transfer of corrective (post-tensioning) forces to the structure. Our approach offers the following advantages over conventional methods of post-tensioning: (1) ease and expedience of implementation, noting that electrical resistance heating of shape memory rods can be accomplished using an electrical generator; (2) reduced losses of post-tenioning force due to such effects as slip and elastic deformations, noting that strains far greater normal elastic strains of steel or composites can be recovered by the shape memory effect; (3) the system retains its capability to correct future damages to the structure, noting that damaging effect would elongate the shape memory rods and such elongations can be recovered simply by electrical resistance heating of the rods.

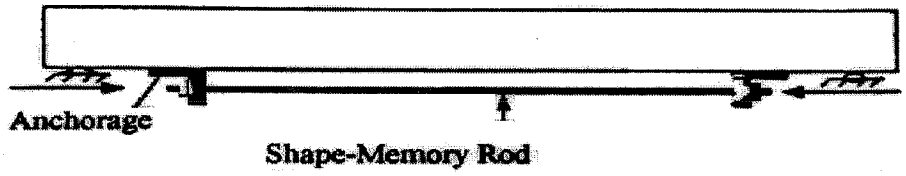

Figure 2. Application of Corrective Forces through Constrained Recovery of Shape Memory Rods.

The project reported herein is the continuation of an NCHRP-IDEA program where the feasibility of our approach to rehabilitation and strengthening of bridge structures was verified through laboratory experiments, and structural design procedures for repair and strengthening of reinforced concrete systems through post-tensioning with shape memory rods were developed.

1.2 OBJECTIVES

The main thrust of the investigation reported here was to verify the feasibility and advantages of shape memory-based rehabilitation technology in field application to bridge structures. The bridge selected for demonstration of the technology has suffered cracking as a result of faulty structural design practices. The shape memory-based rehabilitation system was used to locally strengthen this bridge structure. The project accomplished the following objectives: (1) selection and characterization of low-cost shape memory alloys based on iron for use in post-tensioning of bridge structures; (2) final design and detailing of the shape memory-based rehabilitation system for transfer of corrective forces to bridge structures; (3) laboratory verification of system behavior through tests on scaled structural models; and (4) field implementation of the shape memory-based rehabilitation system.

2.0 SELECTION AND CHARACTERIZATION OF IRON-BASED SHAPE MEMORY ALLOYS

2.1 COMPOSITION OF IRON-BASED SHAPE MEMORY ALLOYS

The iron-based shape memory alloys investigated in this project were as follows:

1. Fe-28%Mn-6%Si-5%Cr manufactured by Nippon Steel Corporation
2. Fe-18%Mn-8%Cr-4%Si-2%Ni-0.36%Nb-0.36%N developed through cooperative work of DPD, Inc. and Oak Ridge National Laboratory

Both above alloys are highly corrosion-resistant.[2-6] The first one is commercially available while the second one was developed through our collaboration with Oak Ridge National Laboratory for increasing the level of constrained recovery force. A major advantage of these alloys is that they can be pre-elongated and stored at ambient temperature; after application and electrical resistance heating for post-tensioning of structural systems, they can again be allowed to cool down to ambient temperature without adverse effects on their post-tensioning forces.

2.2 CHARACTERIZATION OF IRON-BASED SHAPE MEMORY ALLOYS

Iron-based shape memory wires were subjected to 3% pre-strain over a free length of 125 mm at a temperature of 22°C; the stress required for pre-straining of iron-based alloys was of the order of 1000 MPa. The pre-strained (and unloaded) wire was then restrained against shortening (Figure 3) and then subjected to electrical resistance heating to reach a temperature of 300°C. The (restrained recovery) force developed upon cool-down was measured. The effects of temperature variations between extremes of outdoor conditions on the level of restrained recovery force were also determined (after twelve hours of storage at each temperature).

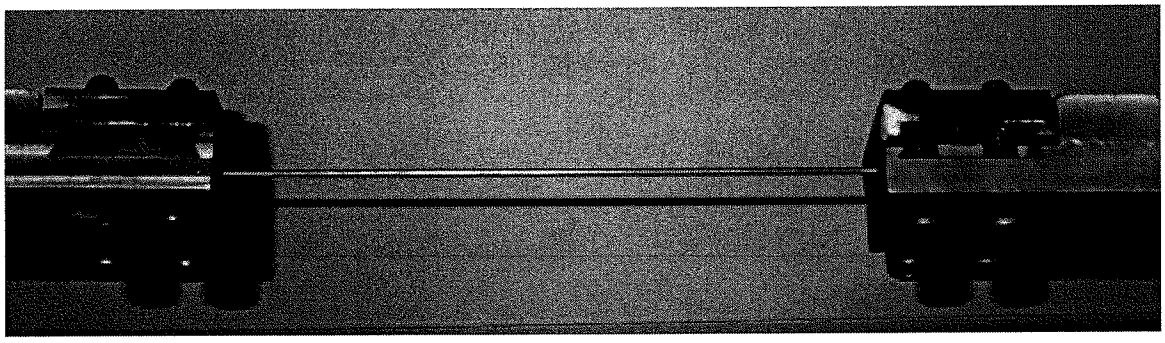

Figure 3. Restrained Recovery Test Set-Up.

The restrained recovery forces developed (after heating to 300°C followed by cool-down to room temperature) by Fe-Mn-Si-Cr and Fe-Mn-Cr-Si-Ni-Nb-N alloys were 255 and 185 MPa, respectively. After re-elongation and re-heating in restrained condition, the alloys could still develop close to 80% of the original recovery force, which confirms their ability to correct future damaging effects on structures (after installation and original activation). Fe-Mn-Si-Cr, which provides higher levels of restrained recovery stress, is selected for post-tensioning of bridge structures.

Figures 4 and 5 depict effects of extreme temperature variations on the restrained recovery stress of the two iron-based shape memory alloys. The restrained recovery force is observed to be minimally affected by extreme temperatures expected in outdoor conditions.

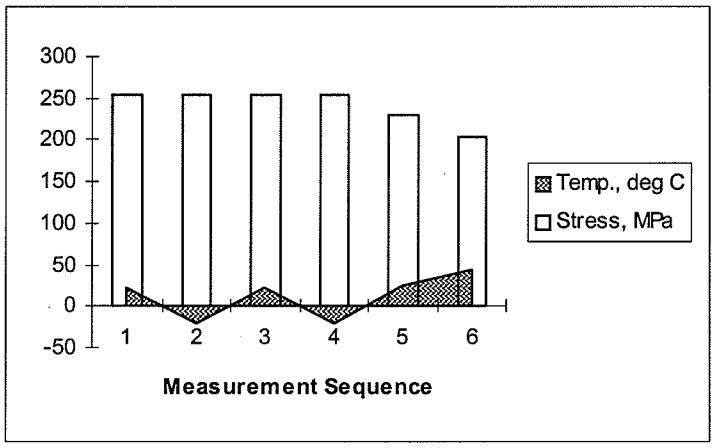

Figure 4. Temperature Effects on the Restrained Recovery Stress of Fe-28%Mn-6%Si-5%Cr.

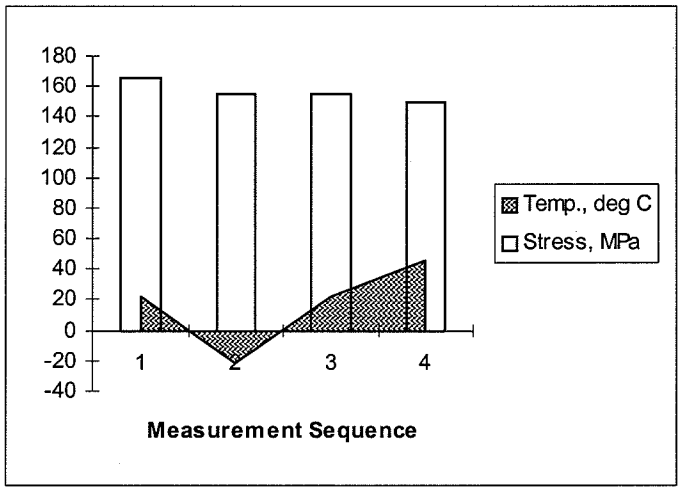

Figure 5. Temperature Effects on the Restrained Recovery Stress of Fe-18%Mn-8%Cr-4%Si-2%Ni-0.36%Nb-0.36%N.

3.0 PRELIMINARY LABORATORY INVESTIGATION OF POST-TENSIONING WITH IRON-BASED SHAPE MEMORY ALLOYS

3.1 INTRODUCTION

Iron-based shape memory alloys provide sufficient strain recovery suiting post-tensioning and repair of reinforced concrete systems. With a cost comparable to that of other steel alloys, iron-based shape memory alloys offer great commercial promise for incorporating some advantages of our technology into reinforced concrete containment systems. The work presented below covers an experimental evaluation of the value of iron-based shape memory alloys in strengthening and rehabilitation of reinforced concrete systems.

3.2 STRUCTURAL DESIGN

The experimental work presented here concerns the corrective effect of the restrained recovery phenomenon in shape-memory alloys on structural elements. For this purpose, a flexural reinforced concrete element damaged under excessive loading was rehabilitated and strengthened through post-tensioning by electrical resistance heating of iron-base shape memory alloys restrained unto the element.

The reinforced concrete beam under investigation is introduced in Figure 6. This beam is reinforced with three W2.0 steel wires in tension (and compression), providing a tension steel area of 26 mm^2. The tensile steel ratio is 0.46%, which is greater than the minimum steel ratio of $200/f_y = 0.33\%$.

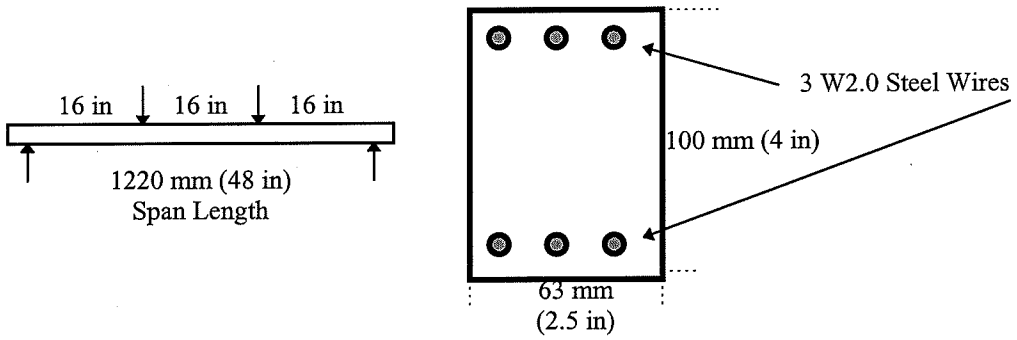

Figure 6. The Reinforced Concrete Beam Under Investigation.

The cross section presented in Figure 6, with 28 MPa (4,000 psi) compressive strength concrete and Grade 60 steel, provides a nominal flexural strength of $9x10^5$N.mm (8,064 lb.in). This implies that the beam, when subjected to four-point loading as shown in Figure 6, fails under a total load of 4,435 N (1,008 lb). The concrete shear strength is so that this beam is safe against shear failure, and thus fails in flexure.

The cracked-transformed moment of inertial of the cross section shown in Figure 6 is $115x10^6$ mm^4 (276 in^4). At ultimate load, assuming an elastic behavior, this yields a deflection of 0.0082 mm (0.0003 in). In the post-yield region, at a mid-span deflection of 5 mm (0.2 in), the strain in tension steel reinforcement at a crack would be 5%. At this level of deflection and steel strain, the beam has already failed and relatively large cracks have developed. Our purpose here is to use the restrained recovery phenomenon in shape-memory alloys to apply corrective forces to the reinforced concrete beam after failure.

Assuming that the shape-memory reinforcement applies eccentric forces at the beam ends (Figure 7), the required restrained recovery force to cause yielding of tension steel in compression (assuming that half of the restrained recovery force would be available to yield the tension steel) is 21,000 N (4,800 lb). This restrained recovery force divided by the restrained recovery stress of a particular shape-memory alloy yields the area of shape-memory rods needed to accomplish this corrective action.

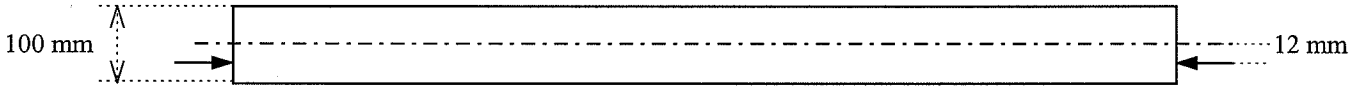

Figure 7. Application of Eccentric Compression for Repair of Elements.

The use of restrained recovery phenomenon for the above purpose, in the case of Fe base shape-memory alloys, involves 3% pre-straining and then unloading of the rods, anchoring them onto the beam, and (electrical resistance) heating of the rods above their transformation temperature for shape recovery (restrained shape recovery in this case) to take place. Restraint of this shape recovery transfers corrective forces to the reinforced concrete element.

3.3 CONSTRUCION OF THE REINFORCED CONCRETE ELEMENT

Figure 8 shows the formwork and reinforcement cage for the reinforced concrete element. Figure 9 shows the process of placing concrete in the formwork; compression specimens were also prepared from concrete to be tested with the beams in order to confirm the targeted compressive strength of 28 MPa (4,000 psi). Finishing of concrete surfaces at the conclusion of specimen preparation is presented in Figure 10. The reinforced concrete elements were moist-cured for two weeks and then air-dried for about six weeks prior to the performance of tests.

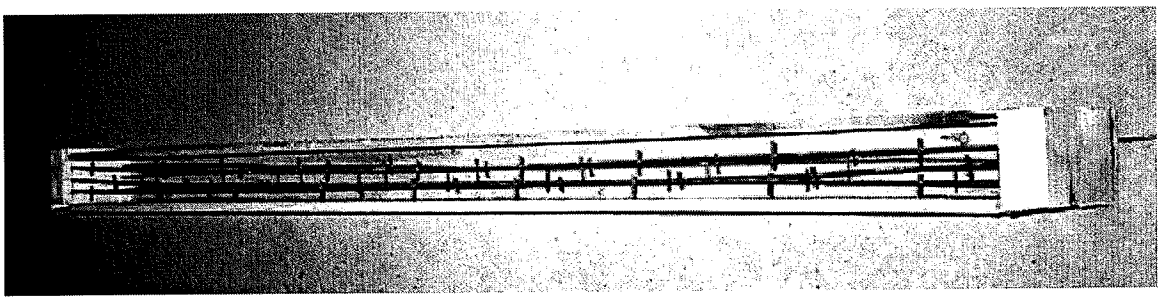

Figure 8. The Formwork and Reinforcement Cage for the Reinforced Concrete Element.

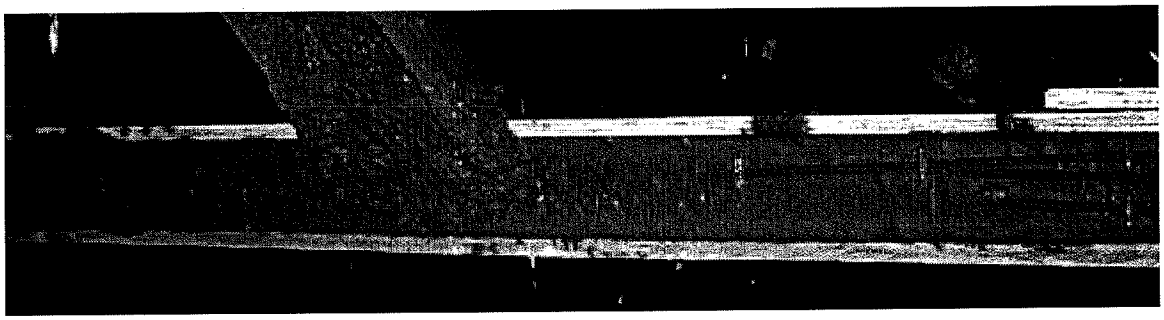

Figure 9. Placement of Concrete in The Formwork.

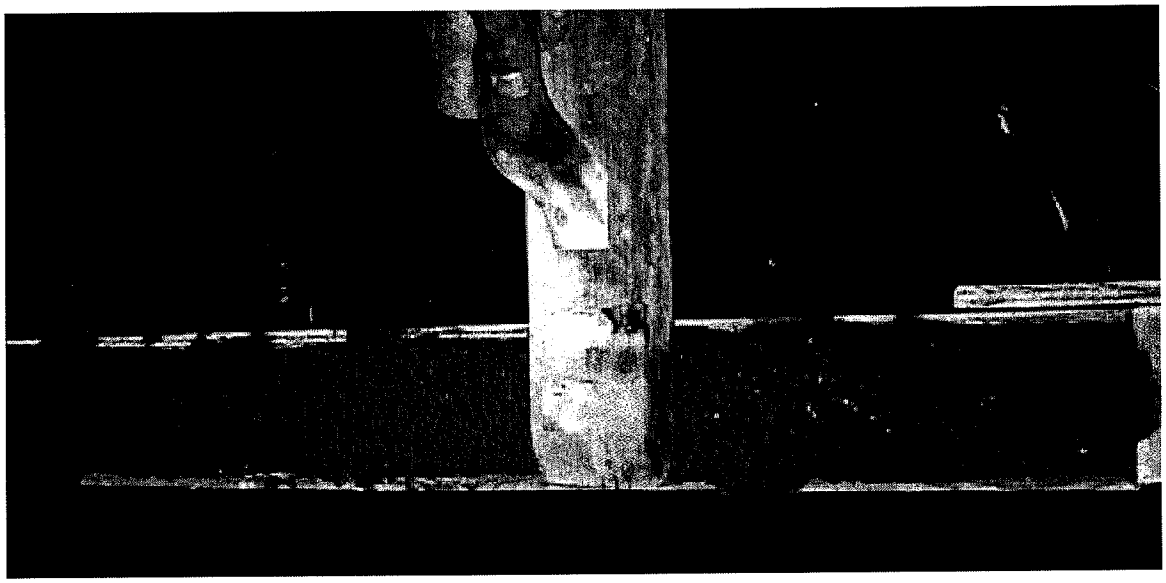

Figure 10. Finishing of the Concrete Surface.

3.4 INITIAL LOADING TO DAMAGE THE ELEMENT

Two of the elements were loaded to a maximum inelastic midspan deflection of about 12 mm and then unloaded. Figure 11 presents a picture of one of the elements under test. Due to yielding of steel reinforcement, the elements developed a permanent deflection. Figure 12 presents a picture of the element after test. The element also developed multiple flexural cracks. The maximum crack width after unloading was 0.2 mm; five cracks could be observed after unloading. The load-deflection curve during loading and unloading is presented in Figure 13. The permanent mid-span deflection is observed to exceed half the maximum deflection reached during the test. The test was quasi-static and the peak load was reached in about 30 seconds.

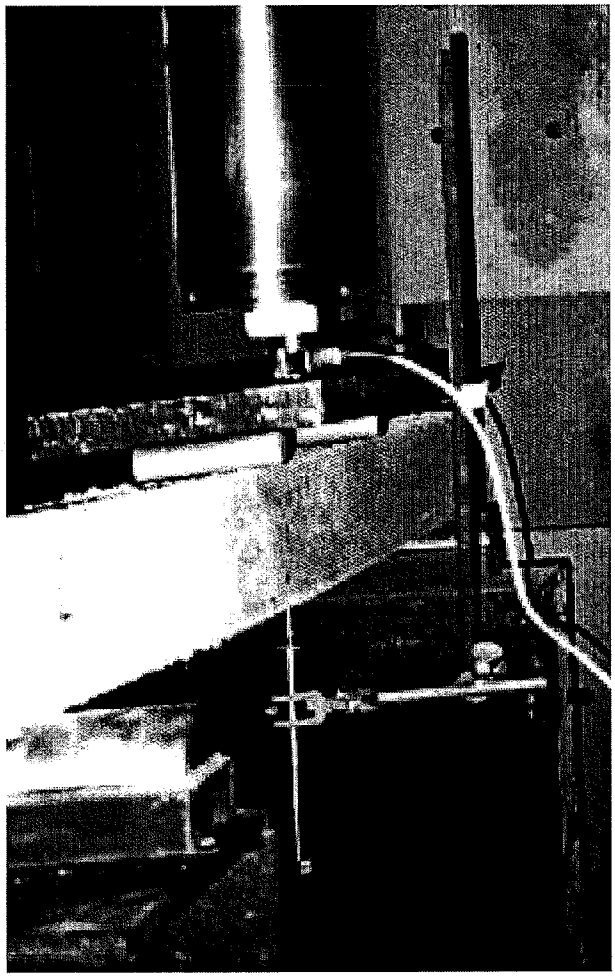

Figure 11. Picture of an Element During Test.

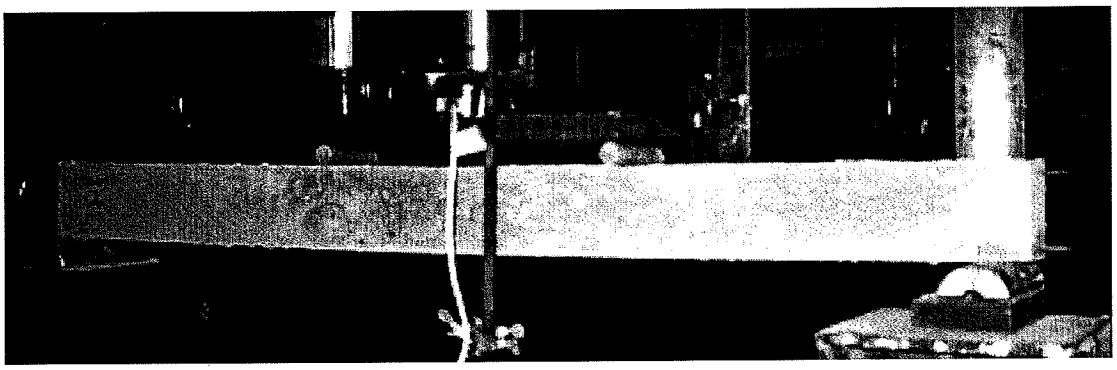

Figure 12. Picture of an Element After Test.

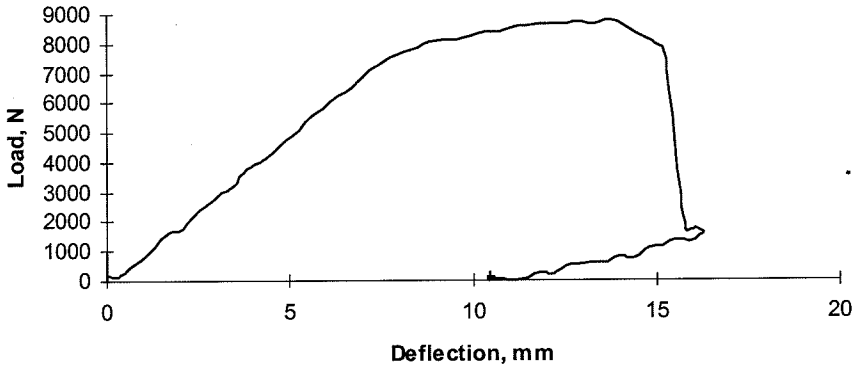

Figure 13. Load-Deflection Relationship for the Reinforced Concrete Element.

3.5 BASIS OF REHABILITATION WITH SHAPE MEMORY EFFECT

The reinforced concrete elements which have sustained permanent deflection and cracking under inelastic loads will be repaired through the application of eccentric compressive loads (Figure 7). The 12 mm eccentricity chosen for the compressive force is below the 16 mm limit beyond which the element develops tensile stresses under eccentric axial compression. The compressive force is 21,400 N. This force is sufficient to cause compressive yielding of the 'tensile' steel reinforcement of the element which has yielded in tension during loading. Since yielding of steel is the reason for permanent deflection and cracking of elements, removal of the permanent elastic deformation in steel would remove the permanent damage of beams.

3.6 REPAIR OF THE DAMAGED ELEMENT BY POST-TENSIONING

We used two 10.4-mm diameter Fe-base shape memory rods to apply corrective post-tensioning forces to the reinforced concrete element. The shape memory rods were subjected to 3% pre-strain at ambient temperature. Figure 14 presents a typical stress-strain curve of rods during application of the 3% pre-strain.

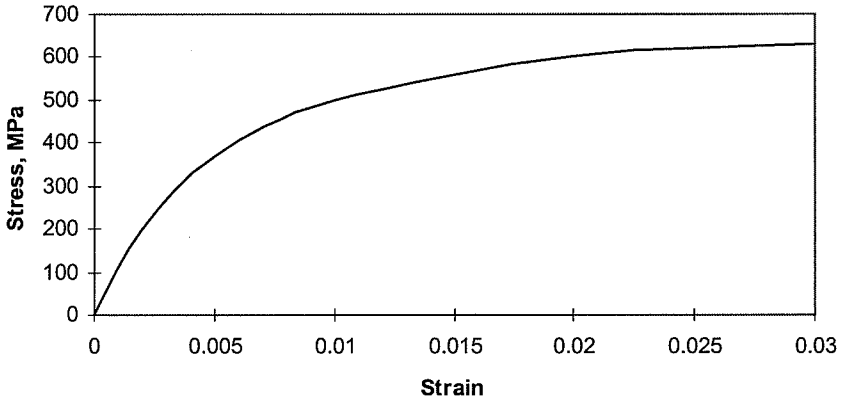

Figure 14. Typical Stress-Strain Curve of the Fe-Base Shape Memory Rod During Application of 3% Prestrain.

Figure 15 presents a picture of the set-up used for the purpose of rehabilitation and strengthening of the reinforced concrete beam. The shape memory rods were threaded and anchored onto a steel rod (to make the whole system longer) and to end plates which bean on the reinforced concrete element.

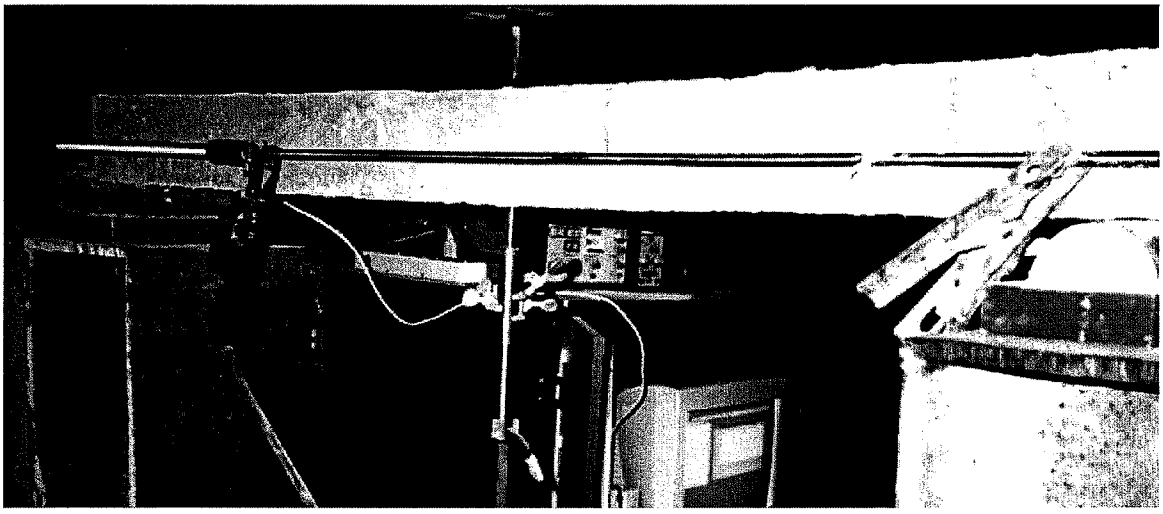

Figure 15. Application of the Strengthening System to the Element.

The shape memory rods were heated sequentially using a welding generator; we were limited to an electrical current of 50A, and could reach the targeted temperature of 300°C after 5 to 10 minutes through simple insulation of shape memory rods. The mid-span deflection (negative represents downward) and the total load applied by restrained shape recovery are presented in Figures 16a and 16b, respectively. Prior to electrical resistance

heating of the shape memory rods for the application of corrective forces, the rods were hand tightened; this is why at time zero the value of force and deflection are not zero. The process of heating of shape memory rods first introduces thermal expansion and then provides for phase transformation shrinkage. This is why at earlier times we observed a loss of (tightening) force before corrective actions associated with an increase in end force and upward movement of the element occurred. The midspan deflection and end force were monitored over a period of few weeks; no noticeable loss of the prestressing force applied by shape memory rods was observed.

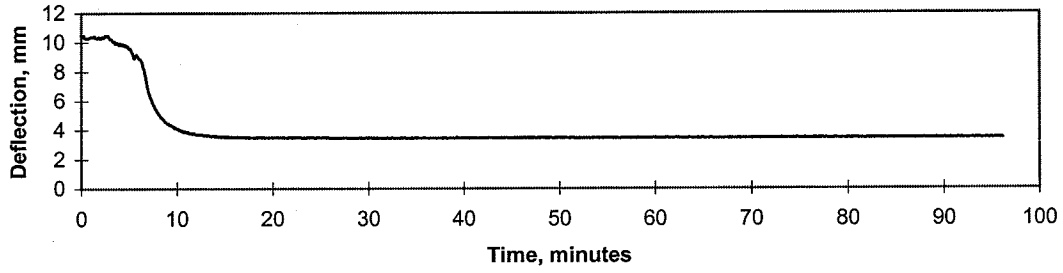

(a) Midspan Vertical Deflection Vs. Time

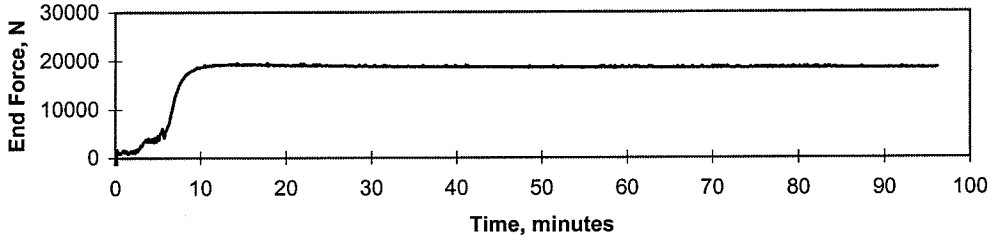

(b) Eccentric Compressive Force at Element Ends Vs. Time

Figure 16. Time-Histories of Midspan Deflection and End Force.

3.7 APPLICATION OF DAMAGING LOADS AND REHABILITATION WITH EXISTING SHAPE MEMORY RODS

The shape memory rods used in the initial post-tensioning effort to rehabilitate and strengthen the element provide unique features for restoration of post-tensioning forces after any losses associated with creep, shrinkage, relaxation, etc., and also for repeated rehabilitation of any future damaging effects by simple electrical resistance heating. The experimental work presented here validates the ability of iron-base shape memory rods to repeatedly apply corrective forces after application of damaging external loads.

The strengthened reinforced concrete element (Figure 17) was subjected to about 12 mm of mid-span deflection through third-point loading, and then unloaded. Figure 18 presents the vertical load-deflection behavior during this process, and Figure 19 shows the relationship between the increase in the end force applied by shape memory rods and vertical mid-span deflection during the loading-unloading process. The beam strengthened with shape memory reinforcement is observed to suffer a relatively small residual displacement after the application and removal of 12 mm of mid-span deflection.

The damaged (previously strengthened) beam was subsequently rehabilitated simply by electrical resistance heating to 300°C of the existing iron-base shape memory rods which were anchored onto the element during the initial rehabilitation process. Figures 20 and 21 shows the changes in mid-span deflection and eccentric end force (applied by shape memory rods), respectively, during this rehabilitation process. This figure shows that residual deflections are largely removed by electrical resistance heating of shape memory rods (after the initial effects of thermal expansion are removed upon cooling of rods), and suggests that existing shape memory reinforcement possesses the ability to repeat its corrective action after damaging effects.

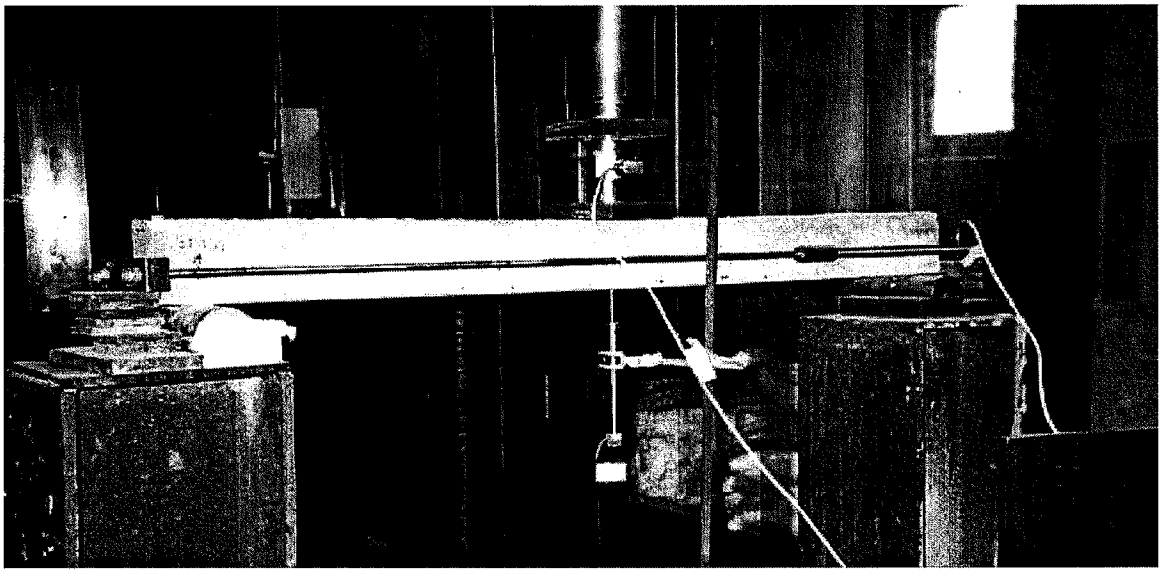

Figure 17. Picture of the Strengthened Reinforced Concrete Element.

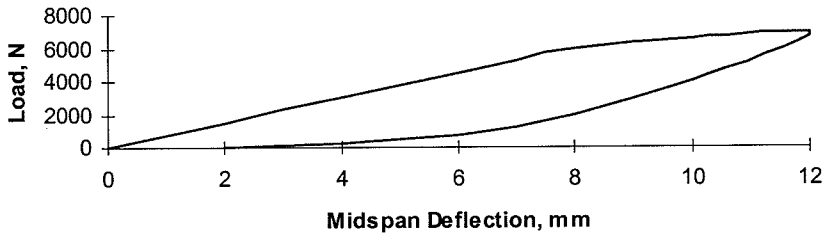

Figure 18. Vertical Load Vs. Midspan Deflection Relationship.

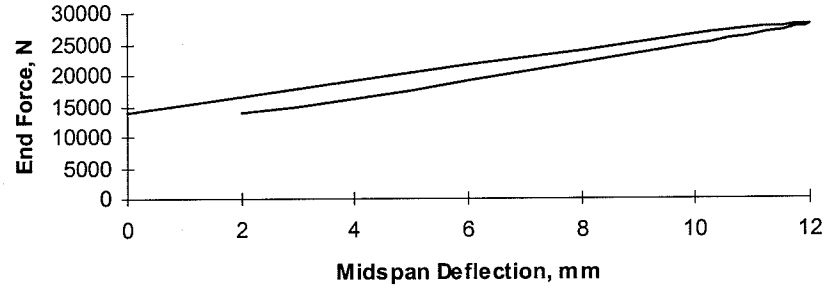

Figure 19. End Force Vs. Midspan Deflection Relatinsip.

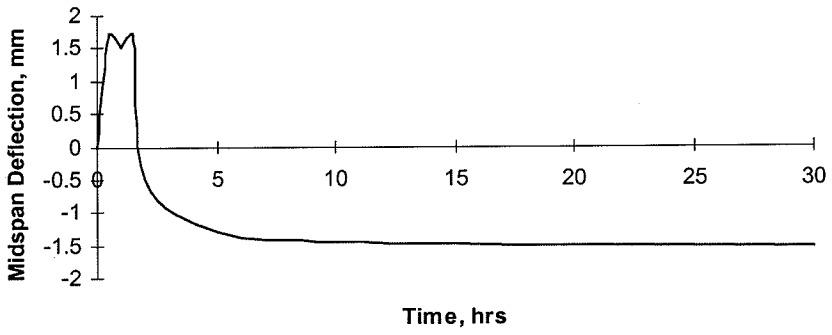

Figure 20. Time-History of Midspan Deflection.

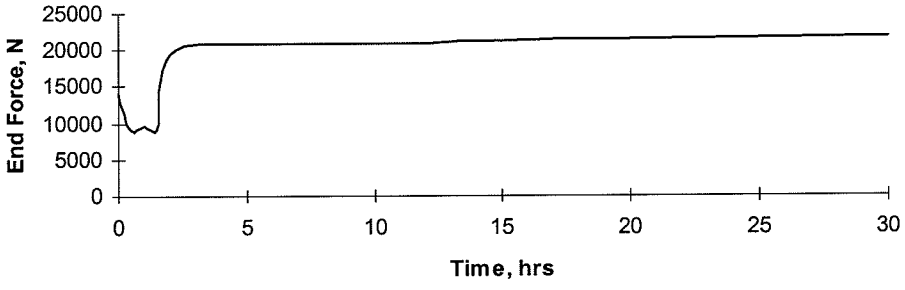

Figure 21. Time History of Eccentric End Force.

4.0 LABORATORY EVALUATION OF REINFORCED CONCRETE ELEMENTS REPRESENTING THE SELECTED BRIDGE CONDITION

4.1 DESCRIPTION OF THE SELECTED BRIDGE STRUCTURE

A picture of the bridge (S03 of 6072, US-31 Under Sherman Road in Michigan) is presented in Figure 22. As shown in Figure 23, the bridge has suffered some cracks in T-beams, extending into the deck. Our focus is on cracks in the negative-moment area of T-beams. These cracks have been attributed, based on an analysis of the bridge under the 11-axle legal truck load weighing 77 tons, to improper cut-off of flexural steel where the shear strength requirements associated with longitudinal bar cut-off are not satisfied. Figure 3 presents a schematic of the longitudinal bar cut-off and crack locations.

Figure 22. An Overall Picture of the Bridge

Figure 23. Picture of a Typical Crack.

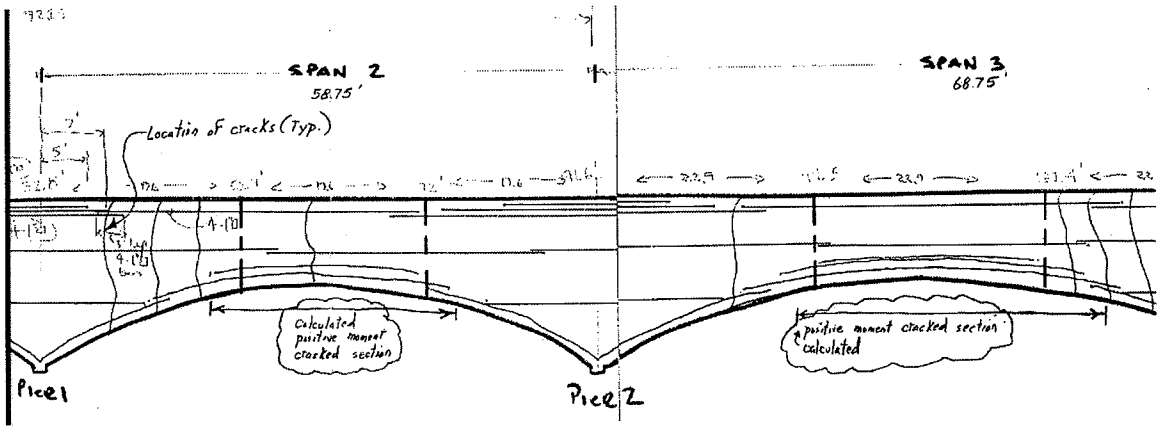

Figure 24. Schematic of Crack and Bar Cut-Off Locations.

4.2 DESIGN OF THE SCALED ELEMENT REPRESENTING THE BRIDGE STRUCTURE

The purpose of post-tensioning with shape-memory rods in the selected bridge structure is to increase shear strength of the beam at the cut-off location of flexural reinforcement in order to meet the shear strength requirements relevant to longitudinal bar cut-off. In an effort to verify this approach in laboratory, we have designed a reinforced concrete beam with longitudinal bar cut-off at a location where the relevant shear strength requirements are not satisfied. Figure 25 presents the reinforced concrete beam design. At the location where the three upper-layer bars are cut off, the total shear strength of the beam is:[7]

$$V_c = (1.9\,(f'_c)^{0.5} + 2500\,\rho_w\,V_u\,.d\,/\,M_u).b_w\,.d \le 3.5\,(f'_c)^{0.5}\,b_w\,.d = 9{,}279 \text{ lb}$$

With #2 stirrups (A_v = 0.1 in^2) of 40,000 psi yield strength provided at 6" spacing, the stirrup contribution to shear strength is 7,667 lb. The total nominal shear strength is thus:

$$V_n = V_c + V_s = 16{,}946 \text{ lb}$$

The nominal flexural strength (M_n) of the beam section shown in Figure 25 with 60,000 psi yield strength of longitudinal steel and 4,000 psi compressive strength of concrete is 16,968 lb.in. The factored mid-span force (P_u) which can be carried, based on flexural strength criteria, by this beam is:

$$P_u = 2\,.(\Phi.\,M_n)/27 = 27{,}799 \text{ lb}$$

The shear force at the longitudinal bar cut-off location under this factored load is 12,870 lb. The required shear strength provided at the bar cut-off location ($\Phi.V_n$ = 0.85 x 16,946 = 14,401) does not exceed this level of shear force by one-third. The shear strength requirements at the longitudinal bar cut-off location is thus not satisfied in this beam (as is the case in the reinforced concrete bridge introduced earlier).

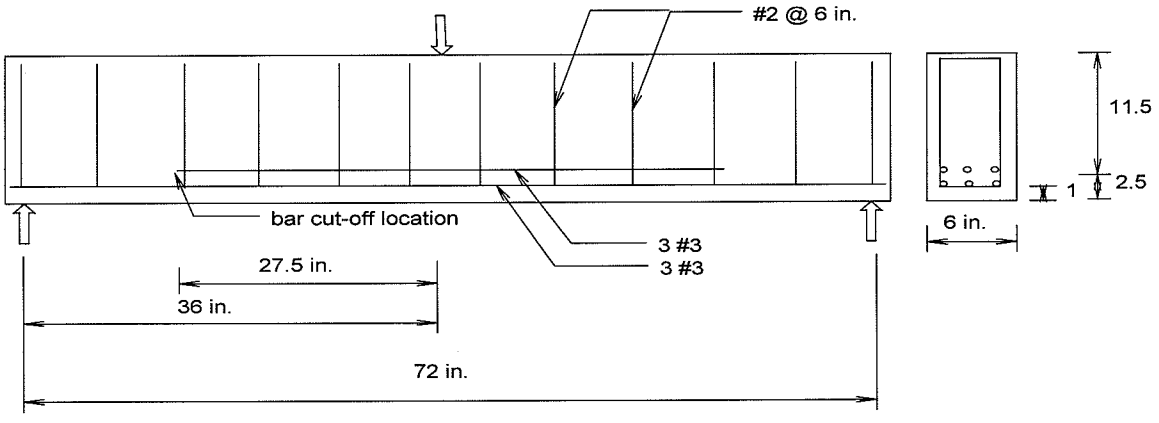

Figure 25. The Reinforced Concrete Beam.

We have selected the post-tensioning set-up presented in Figure 26 for increasing the total shear strength at the longitudinal bar cut-off location by at least 35%. With this post-tensioning scheme using shape memory reinforcement, with two 7,098-lb post-tensioning forces applied at 5.75" distance (centered at bar cut-off point), the total shear strength would be equal to 30,937 lb, which satisfies the shear strength requirement at longitudinal bar cut-off location. In the case of the same shape-memory steel bars introduced for application to the actual bridge, with diameter of 0.41" and restrained recovery stress of 25,000 psi, two bars would be required to apply a post-tensioning force close to the required level of 7,098 lb.

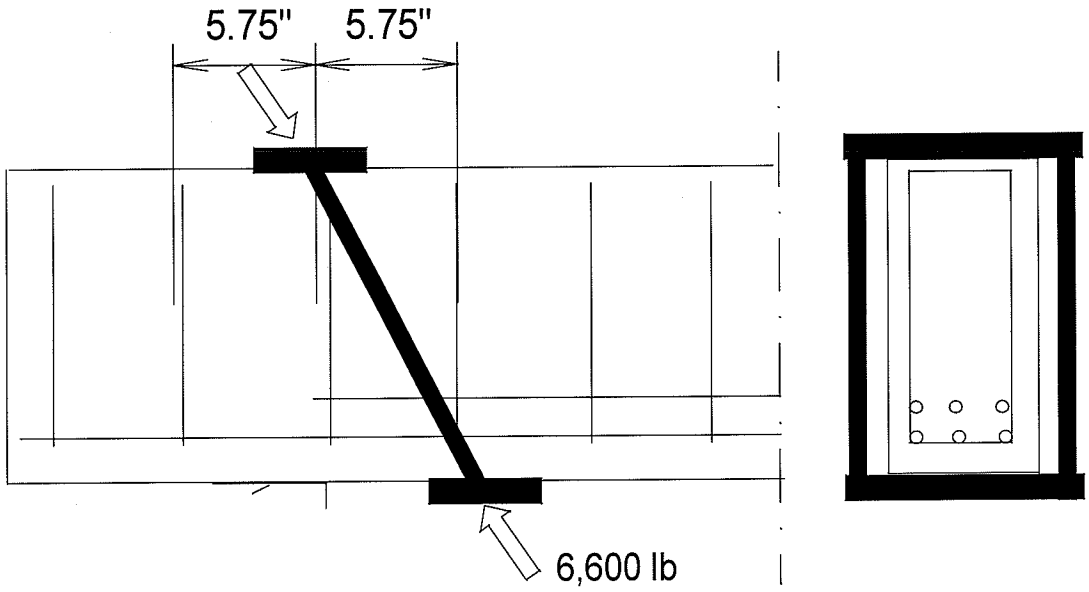

Figure 26. Post-Tensioning Scheme for the Laboratory-Scale Beam.

4.3 PREPARATION & EXPERIMENTAL EVALUATION OF THE SPECIMEN

Figure 27 presents the reinforcement cage used in these beams. A picture of one of the beams is presented in Figure 28.

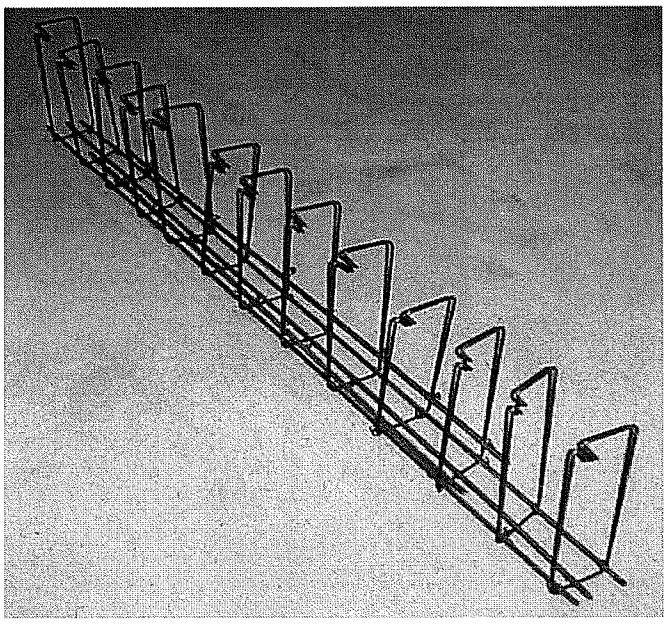

Figure 27. The Reinforcement Cage Used in Reinforced Concrete Beams.

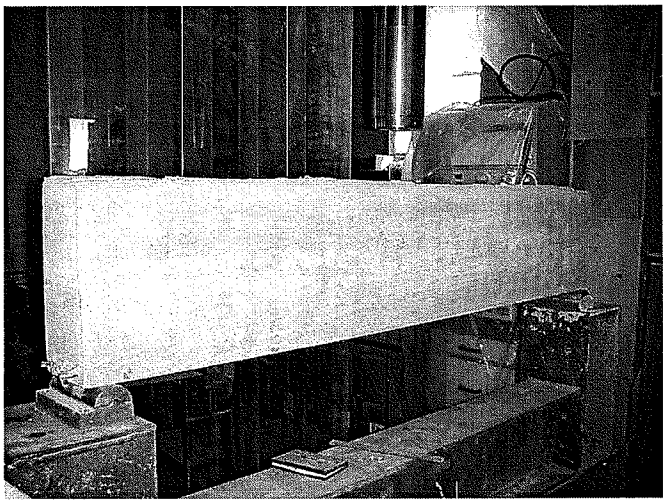

Figure 28. Picture of Beam.

We loaded the beam shown in Figure 28 to cause cracking; subsequently, we repaired the damaged reinforced concrete beam through restraint of shape recovery in shape memory steel rods.

Figure 29 depicts the reinforced concrete beam under initial loading up to the formation of cracks. Shear cracks formed (see Figure 29b), as predicted, at areas where bar cut-off caused concentration of stresses.

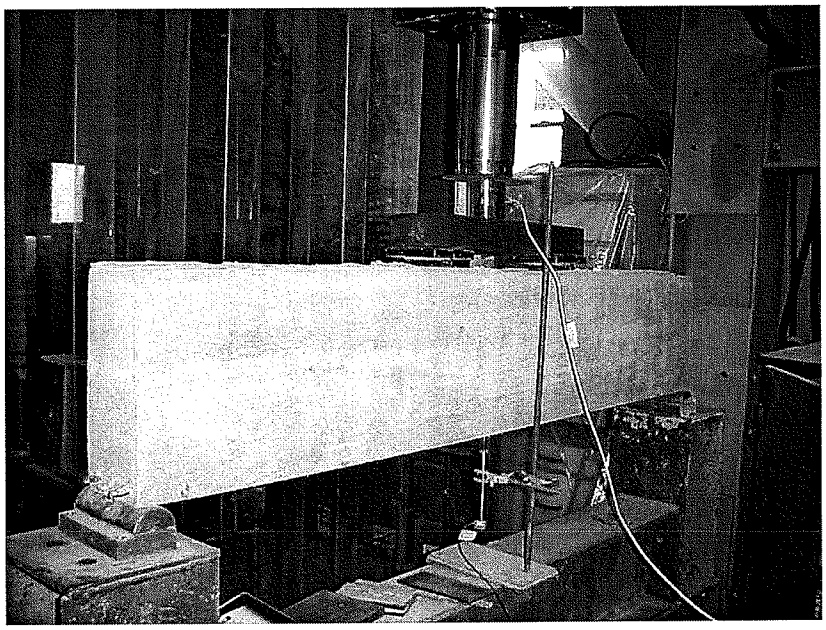

(a) Loading Configuration

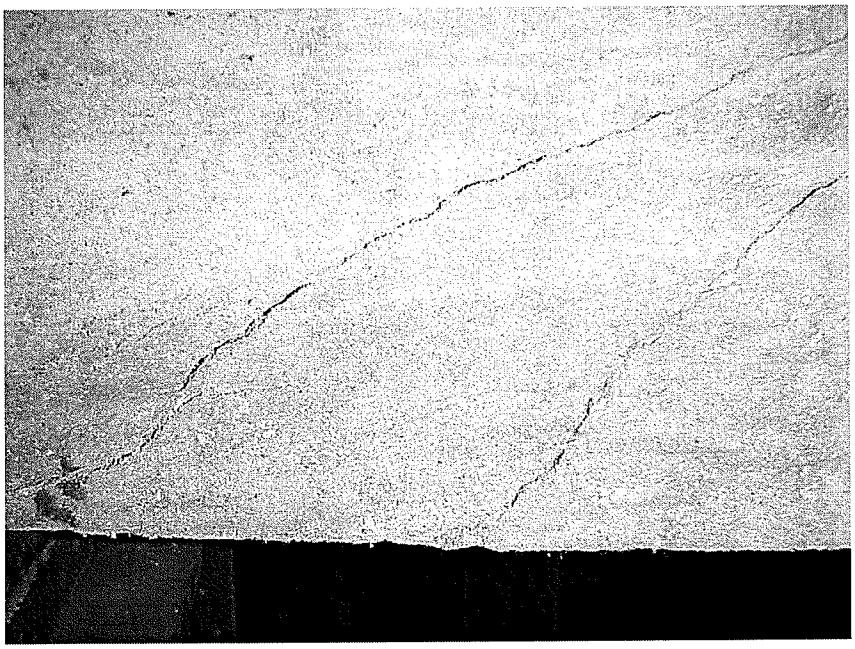

(b) Shear Cracks

Figure 29. Initial Loading of the Reinforced Concrete Beam Up to the Formation of Shear Cracks.

The reinforced concrete beam was subsequently repaired through post-tensioning with shape memory steel rods following the design configuration presented earlier. A picture of the repaired beam is shown in Figure 30.

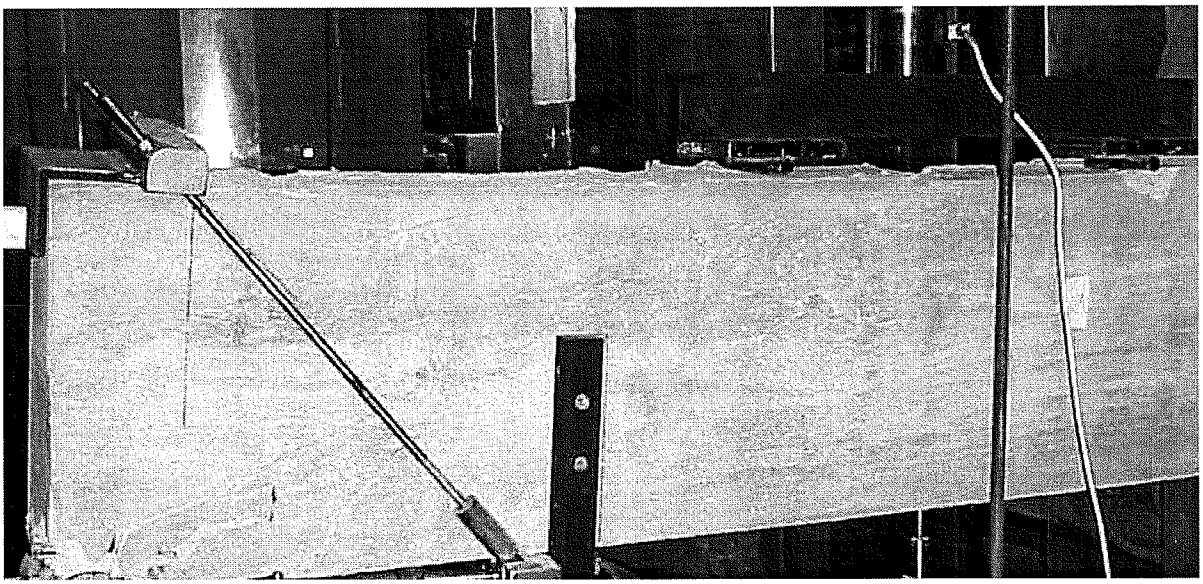

Figure 30. The Repaired Reinforced Concrete Beam.

The repaired beam was then subjected to loading up to failure. Figure 31 presents the load-deflection curve in initial loading of the undamaged reinforced concrete beam. The load-deflection curve after repair is presented in Figure 32. A comparison of Figures 31 and 32 suggests that post-tensioning with shape memory steel was successful in restoring the original load-carrying capacity of the reinforced concrete beam after shear cracking.

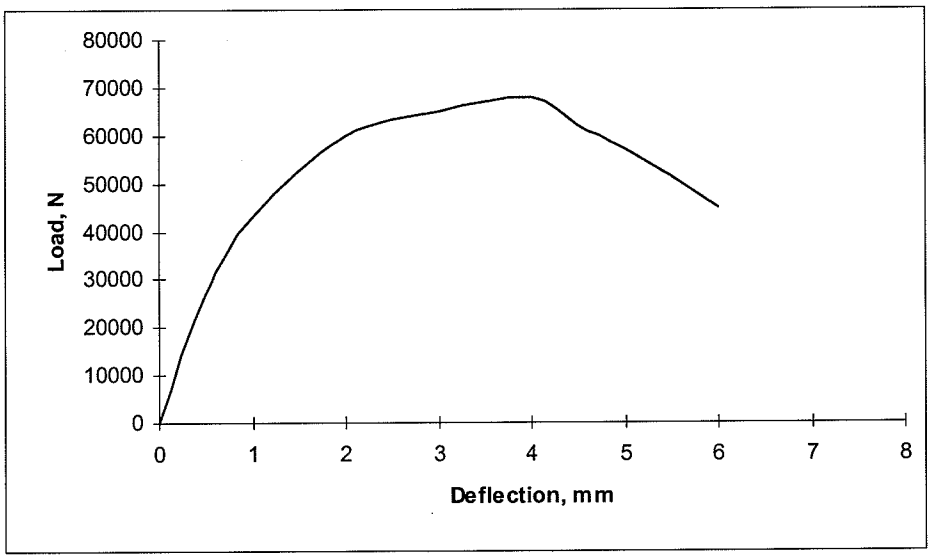

Figure 31. Initial Load-Deflection Behavior of the Undamaged Beam.

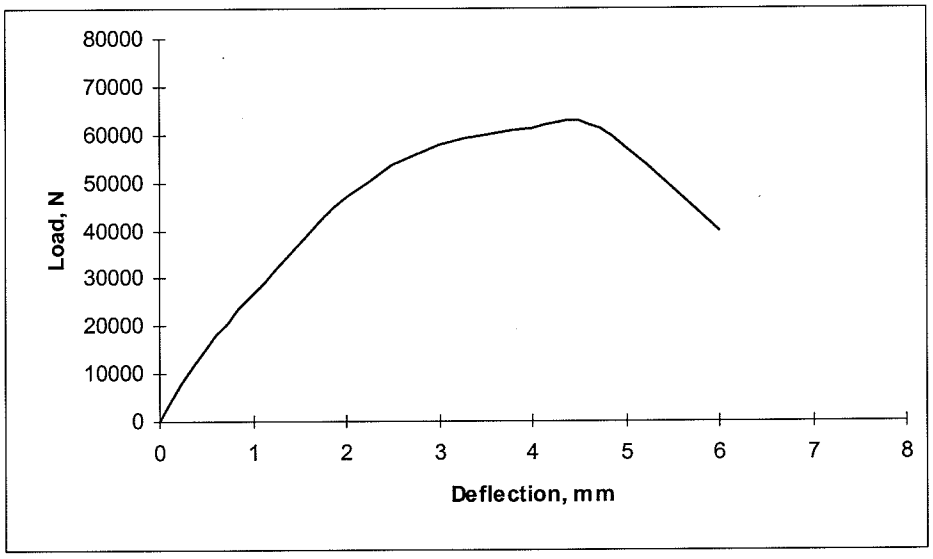

Figure 32. Load-Deflection Behavior of the Reinforced Concrete Beam After Shear Cracking and Repair with Shape Memory Steel Rods.

5.0 DESIGN AND FIELD DEMONSTRATION OF THE TECHNOLOGY IN APPLICATION TO THE SELECTED BRIDGE STRUCTURE

5.1 DESIGN OF THE REHABILITATION SYSTEM

The selected bridge structure was introduced in Section 4.2 (see Figures 22 through 24). Our approach involves local post-tensioning of the cracked region (Figure 33) to increase the shear strength of T-beams to the level satisfying the requirements associated with longitudinal bar cut-off. This requirement essentially requires one-third extra shear strength to resist cracking caused by stress concentrations associated with bar cut-off.

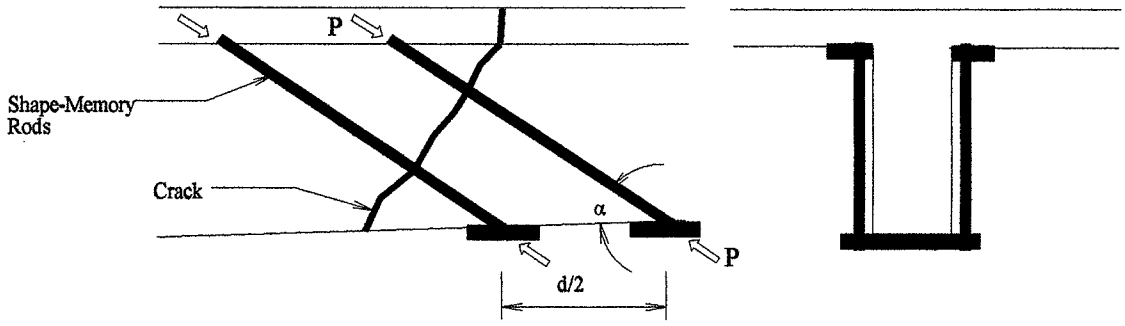

Figure 33. Schematics of Local Post-Tensioning for the Enhancement of Shear Resistance.

The magnitude of prestressing force (P in Figure 33) has to be selected to provide the reinforced concrete beam with on-third (we have chosen 35%) extra shear strength. Our analysis focuses on the crack that is closest (at a distance of about 100 in.) from pier 1 (see Figure 24). The shear strength of the beam strengthened through external post-tensioning (Figure 33) would be governed either by flexure-shear strength (V_{ci}) or web-shear strength (V_{cw}):

$$V_{ci} = 0.6\, b_w \,.\, d \,.\, (f'_c)^{0.5} + V_d + V_i \,.\, M_{cr} / M_{max} + P \,.\, \sin(\alpha) \,.\, \cos(\alpha - 45)$$

$$V_{cw} = [3.5\, (f'_c)^{0.5} + 0.3\, f_c) \,.\, b_w \,.\, d + V_p$$

where, b_w = web width = 18"
d = effective depth = 47"
f'_c = concrete compressive strength = 3,500 psi
V_d = shear force caused by self-weight = 22,050 lb

M_{max} = maximum moment at the section
V_i = shear force corresponding to M_{max}
M_{cr} = cracking moment of the beam = 4,450,639 + 38.9 P cos(α)
f_c = concrete stress due to prestressing = P.cos(α) / (b_w.d/2)
V_p = vertical component of the prestressing force = P.sin(α)

The following values are obtained by the application of the above equations to the reinforced concrete beam in the selected bridge:

$$V_{ci} = 52{,}080 + [4{,}450{,}680 + 38.9\ P\cos(\alpha)].V_i/M_{max} + P\sin(\alpha)\cos(\alpha\text{-}45)$$

$$V_{cw} = 175{,}122 + 0.6\ P\cos(\alpha) + P.\sin(\alpha)$$

The smaller of the above values would be the nominal shear strength provided by concrete. For the case $\alpha = 45^\circ$, one arrives at the following expressions:

$$V_{ci} = 52{,}080 + (4{,}450{,}680 + 27.5\ P).\ V_i/M_{max}$$

$$V_{cw} = 175{,}122 + 1.13\ P$$

The reinforced concrete beam shear strength (V_n) is the sum total of the concrete (V_c, that is the smaller of V_{ci} and V_{cw}) and stirrup (V_s) contributions to shear strength:

$$V_n = V_c + V_s$$

Our analysis focuses on the crack that is closest (at a distance of about 100 in.) from pier 1 (see Figure 24). The nominal shear strength is 175,122 lb prior to strengthening through post-tensioning. We finally chose an angle of 35° for shape memory rods (see Figure 34) so that all holes drilled into concrete web would be located below the neutral axis in compression zone. In order to increase the nominal shear strength of the beam by 35%, one requires a post-tensioning force (at 35° angle) of 74,787 lb (in the worst case scenario where V_i/M_{max} exceeds 0.024 and thus V_{cw} governs the design). The 35° angle of shape memory rods was selected in order to avoid drilling holes in tensile regions of the beam (see Figure 34).

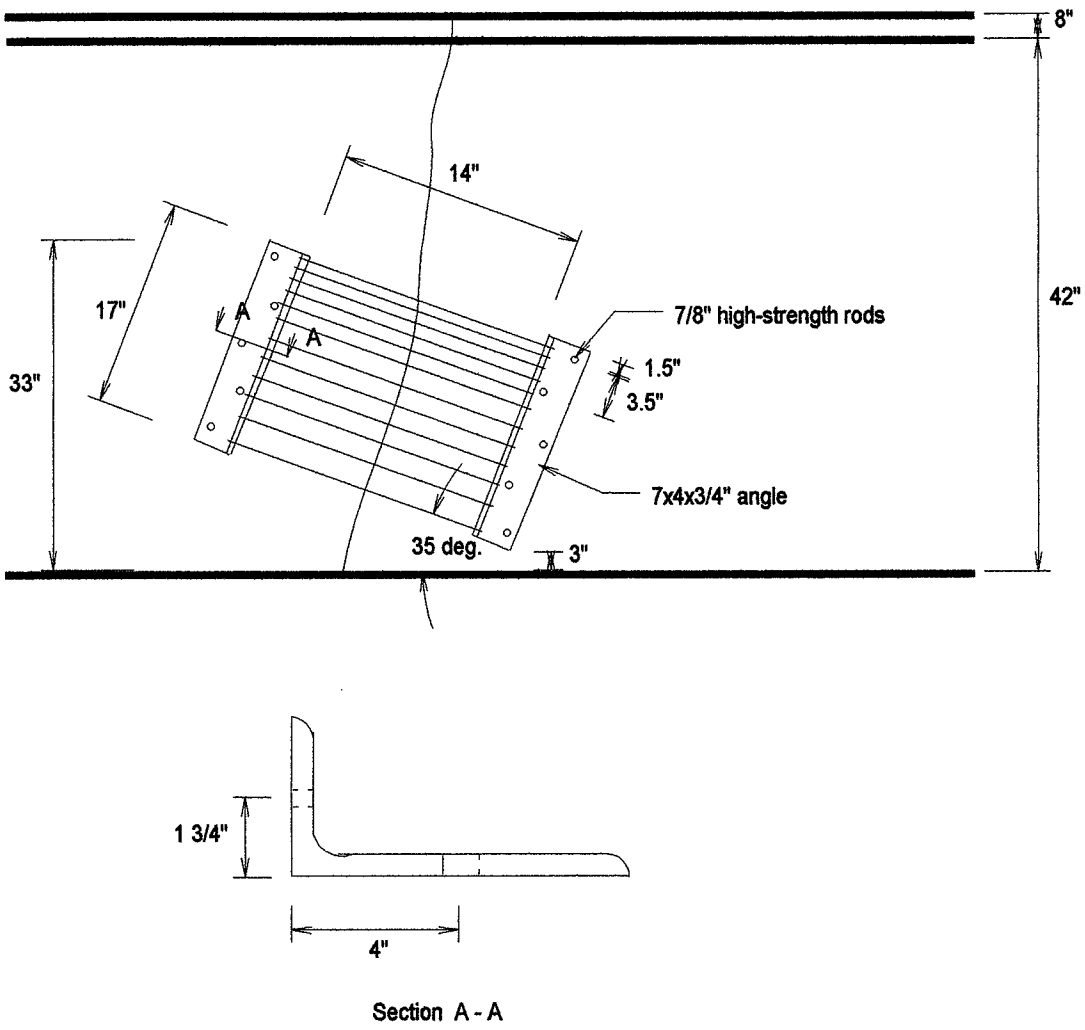

Figure 34. The Final Configuration of Shape Memory Rods.

The 24 shape memory rods (with 0.41" diameter) apply a post-tensioning force of 24x3,300=79,200 lb to the beam. The anchorage design consisting of five 7/8" diameter high-strength rods connecting the angle to the web should transfer this force to concrete. The following checks confirm adequacy of this anchorage system.

Bearing Strength of Concrete = (79,200)/(5x7/8x18) = 1,005 psi < 0.3 f'_c = 1,056 psi √

Bolt Shear Stress = [(79,200)/(5x2)]/[$\pi(7/8)^2/4$] = 13,171 psi < 19,000 psi √

Bolt Bearing Stress = 7,920/(7/8x3/4) = 12,068 psi < 20,000 psi (AASHTO) √

Bolt Tensile Stress = (39,600x1.75/4)/[$5\pi(7/8)^2/4$] = 5,762 psi < 36,000 psi √

Angle Flexural Stress = 39,600x1/[17x$(3/4)^2/6$] = 24,847 psi ~ 20,000 psi √

Angle Shear Stress = 39,600/[(17-12/2)x3/4] = 4,800 psi < 12,000 psi √

Angle Tensile Stress = 39,600/[(16-5)x3/4] = 4,800 psi √

The anchorage for the final system design of Figure 34 thus satisfies the relevant design requirements.

5.2 FIELD IMPLEMENTATION AND EVALUATION OF TECHNOLOGY

The reinforced concrete bridge (S03 of 61072m YS-31 Under Sherman Road) which is subject of the filed demonstration project is depicted in Figure 35. As noted earlier, the reinforced concrete girders in this bridge lacked sufficient shear strength at the longitudinal bar cut-off locations; this condition led to cracking of girders (Figure 36).

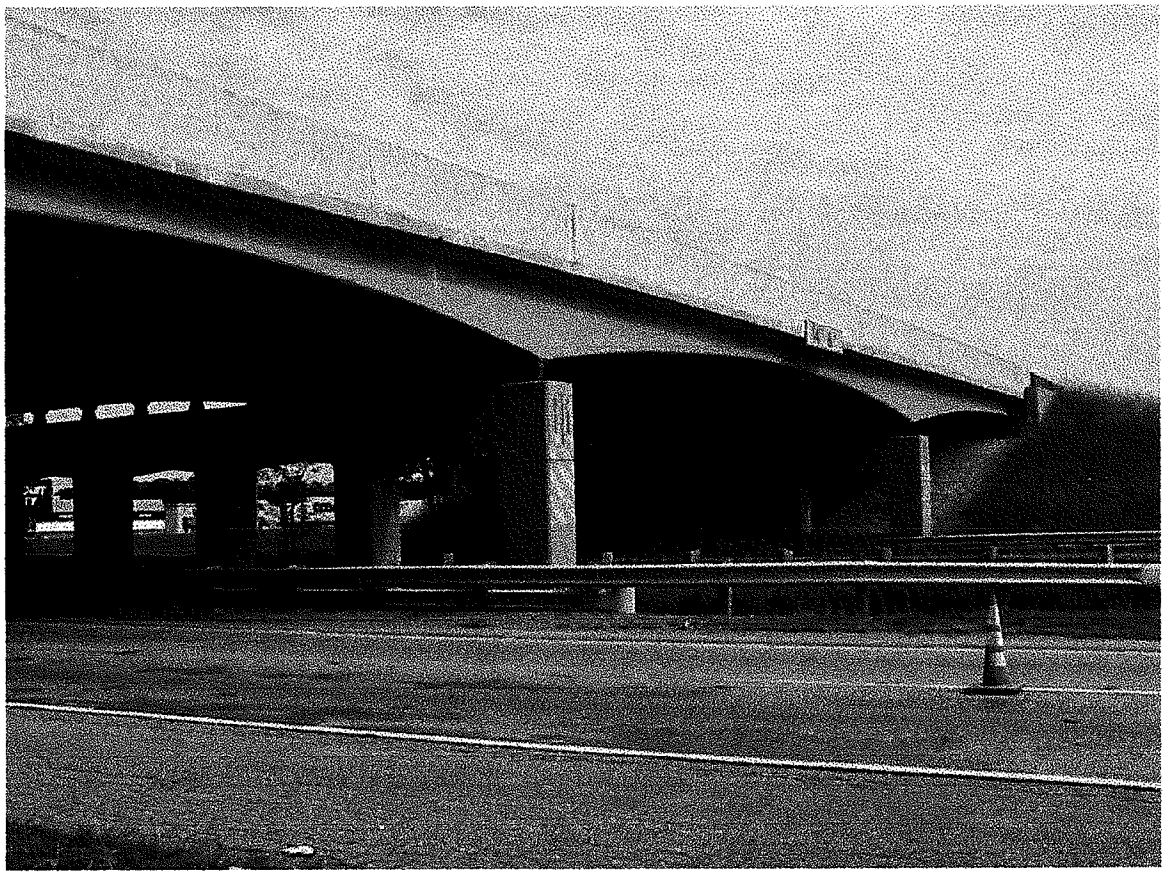

Figure 35. Overall View of the Bridge Structure.

Figure 36. Cracks in Reinforced Concrete Girders.

Based on the design presented earlier (see Figure 34), the process of strengthening the cracked areas through post-tensioning comprised the steps of:

1. Drilling of holes through the girder web for anchoring angles
2. Anchorage of the angles onto the web
3. Anchorage of shape memory rods subjected to 3% pre-strain to angles
4. Electrical resistance heating of the end plates to apply post-tensioning forces through the tendency towards shape recovery

Following the design presented in Figure 34, the first step in implementing the field project involved drilling holes into the girder web (Figure 37). This step was followed by the anchorage of angles onto the web (Figure 38).

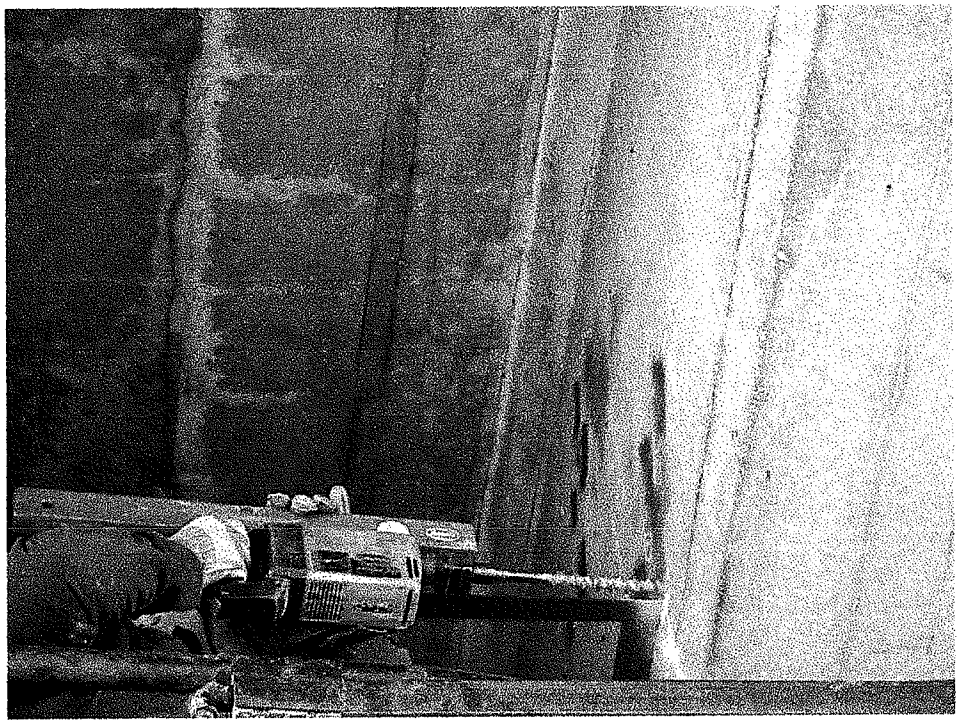

Figure 37. Drilling of Holes in the Girder Web.

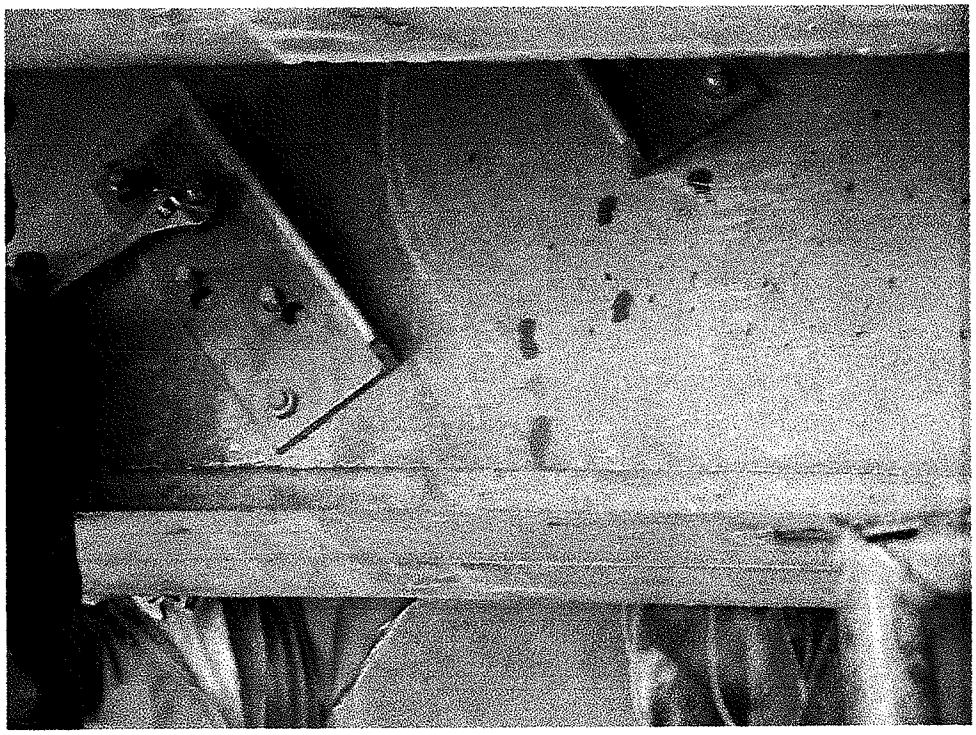

Figure 38. Anchorage of Angles Onto the Web.

The next step in the process involved anchorage of the pre-strained shape-memory rods onto the angles (Figure 39). This was followed by electrical resistance heating of the shape memory rods (Figure 40) in order to prompt the tendency towards shape recovery which, due to the restrained condition of rods, applies post-tensioning forces to the web. Electrical resistance heating of the rods was accomplishing using 100A current (Figure 41), targeting a temperature of 300° C (Figure 42).

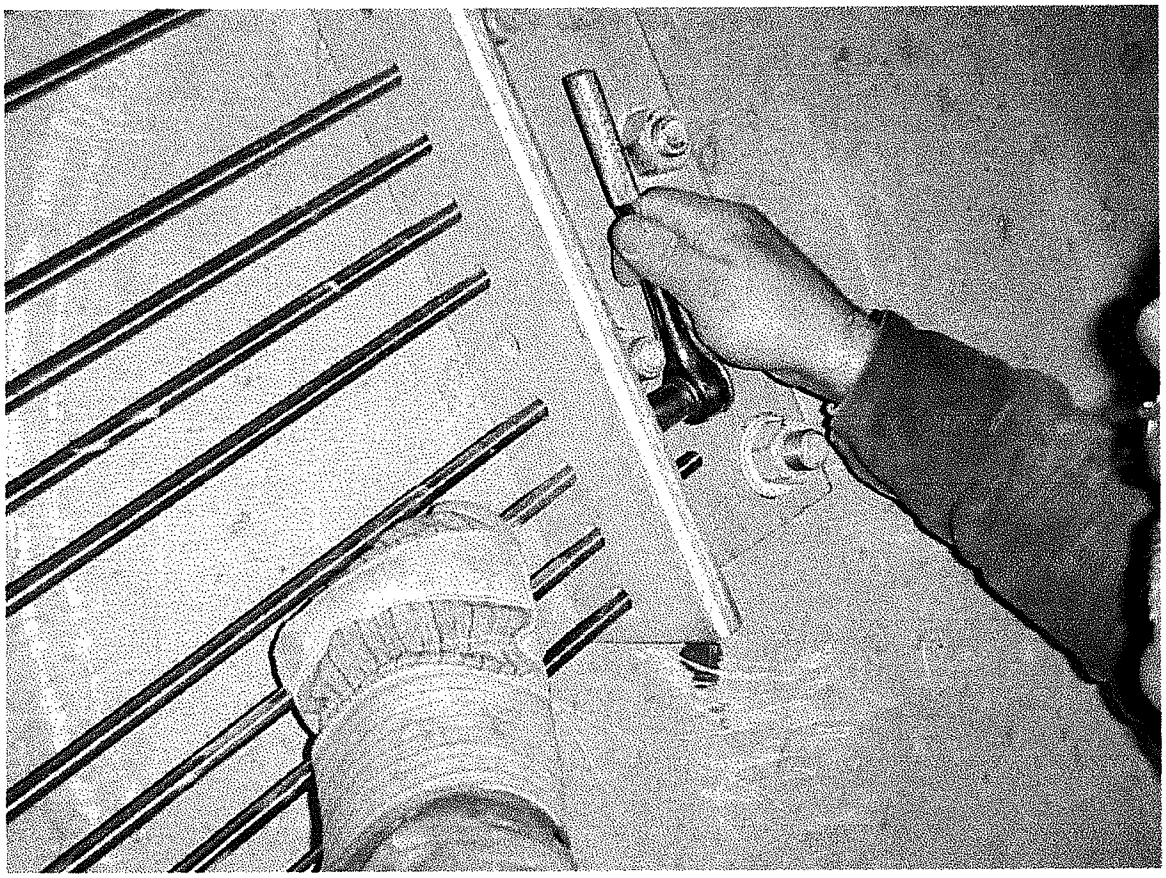

Figure 39. Anchorage of the Pre-Strained Shape Memory Rods to Angles.

Figure 40. Electrical Resistance Heating of the Shape Memory Rods.

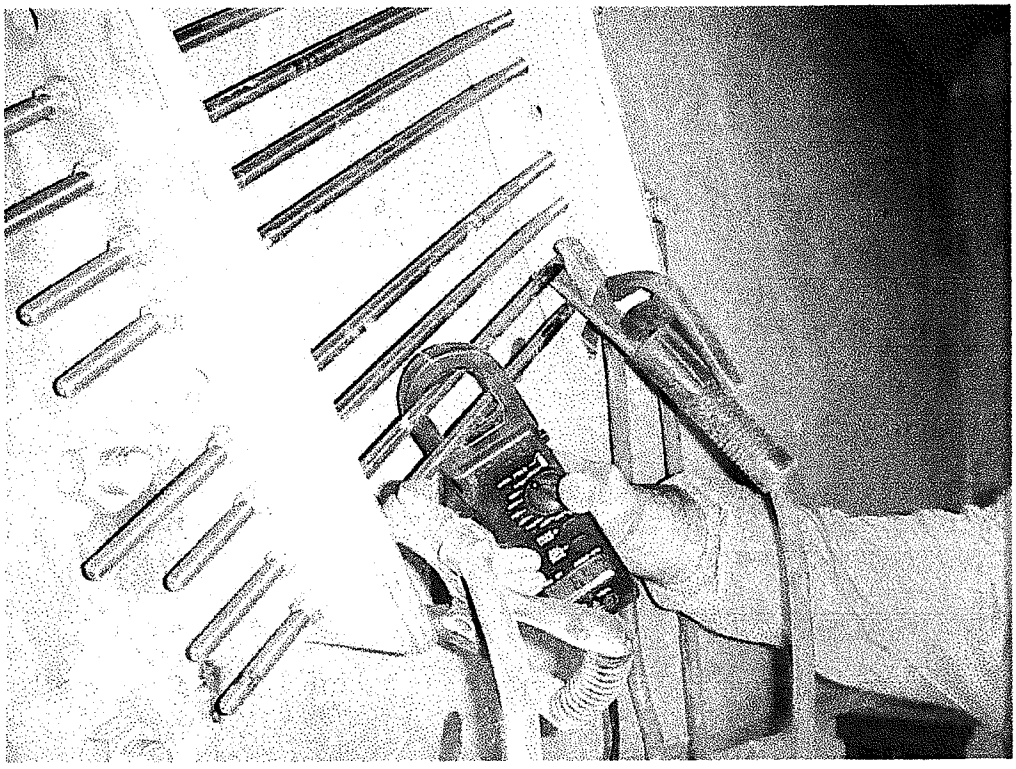

Figure 41. Measurement of Electrical Current During Heating of Shape Memory Rods.

Figure 42. Measurement of Temperature During Heating of Shape Memory Rods.

The final set-up, after post-tensioning through electrical resistance heating, is shown in Figure 43. Both faces of the web received the set-up shown in this figure.

Figure 43. The Final Set-Up.

5.3 MEASUREMENTS MADE DURING THE FIELD PROJECT

Two series of measurements were made during implementation of the field project. The crack width which was focus of the field project was measured prior to (Figure 44) and after (Figure 45) post-tensioning with shape memory rods. Also, the post-tensioning forces of one rod were measured throughout electrical resistance heating and subsequent natural cooling of the rod.

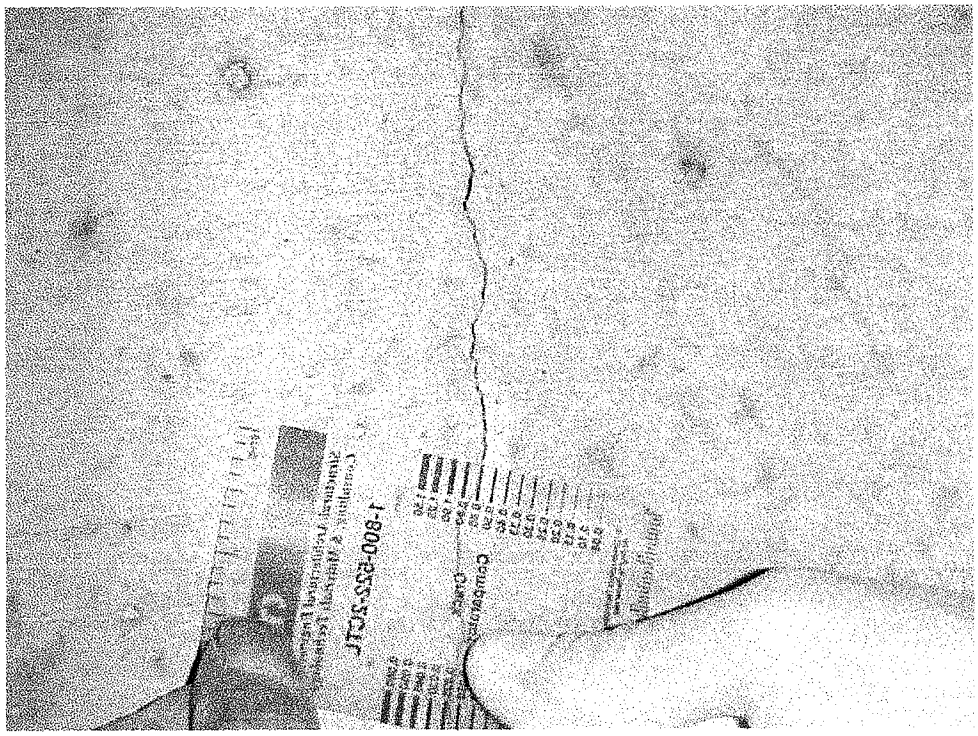

Figure 44. Crack Width Measurement Prior to Post-Tensioning.

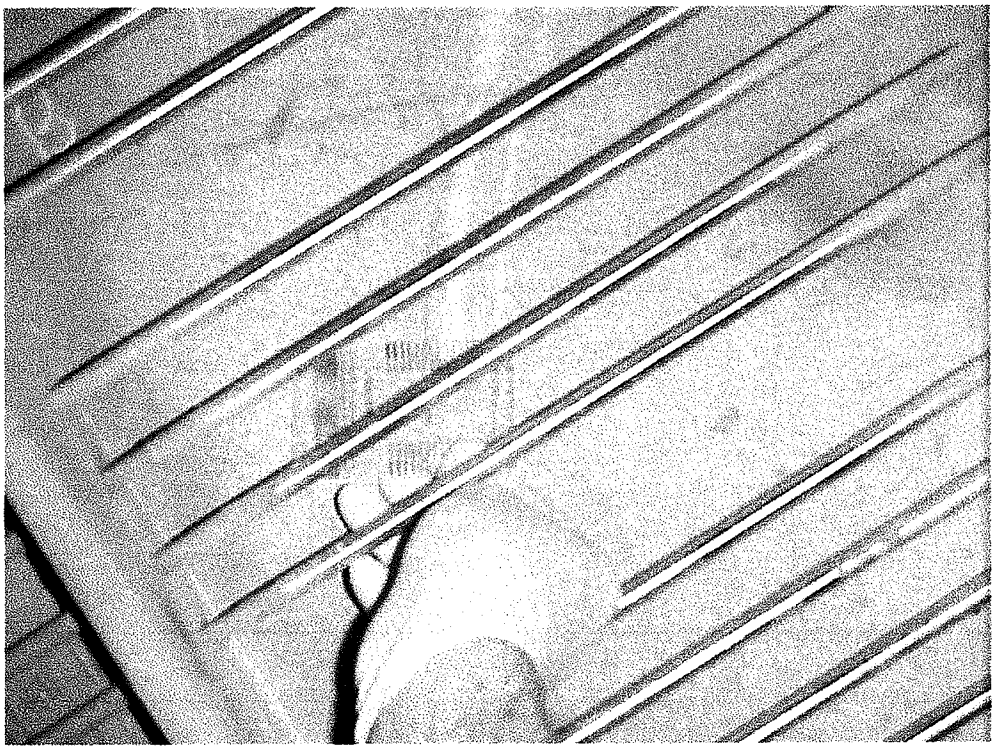

Figure 45. Crack Width Measurement After Post-Tensioning.

The Average crack width, based on three measurements (at top, mid-height and bottom of the web), prior to post-tensioning was 0.55 mm. Post-tensioning reduced this average crack width by about 40% to 0.32 mm. Figure 46 shows the time-history of forces applied by one shape memory rod throughout the process of electrical resistance heating followed by natural cooling. The restrained shape recovery force applied by one rod approaches 10,000 N upon natural cooling. This force level indicates that the shape memory rods of 10.4 mm diameter developed a post-tensioning stress of 120 MPa (17 ksi).

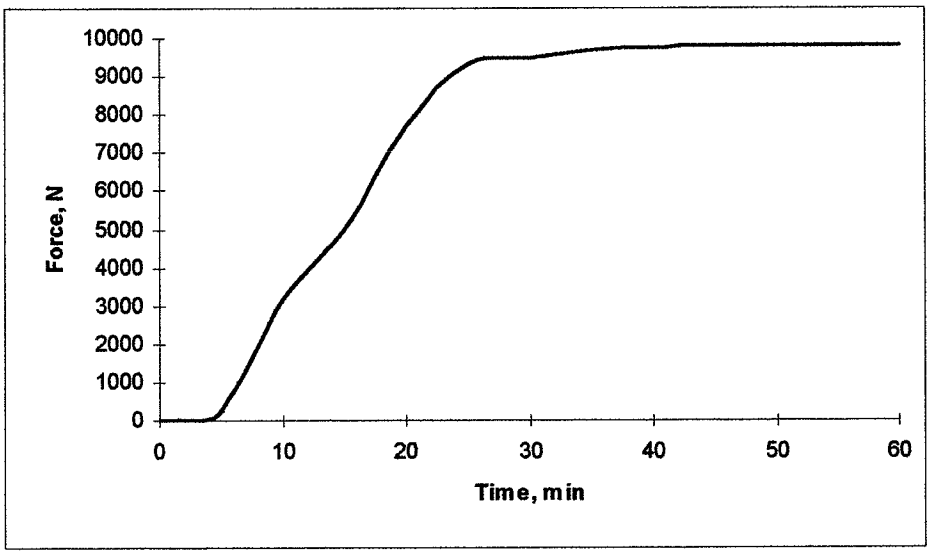

Figure 46. Time-History of the Restrained Shape Recovery Force Applied by One Shape

5.4 LESSONS LEARNED FROM THE FIELD EXPERIENCE

The field project reported above provided us with valuable experience in design and implementation of shape memory-based system for the application of corrective forces to deficient (or damaged) structural systems. The project demonstrated advantages of the approach in terms of convenience and speed of implementation. The strengthening effects with shape memory rods were accomplished without adding any noticeable dead weight to the structure. We also gained substantial experience in anchoring shape memory rods to reinforced concrete structural systems under constrained field conditions. The only major problem encountered in this particular field project related to the difficulty of predicting the exact location of reinforcing bars within reinforced concrete beams. Occasionally, we had to shift the angle holes and enlarge the holes drilled into the reinforced concrete beam (Figures 37 and 38) in order to avoid reinforcing bars. This allowed for relatively large slippage at end anchorages of shape memory rods, which reduced the level of restrained recovery stress developed in them. Hence, the bars

developed 120 MPa (17 ksi) stress as compared with the targeted stress level of 176 MPa (25 ksi). The relatively large recoverable strain of shape memory steel (about 2%) was a positive factor here; otherwise, the whole post-tensioning force could be lost due to the large slippage of end anchors. Also, due to the geometric constraints resulting from shifts in bolt locations, only ten shape memory rods could be anchored onto each face of the beam (in lieu of the targeted twelve bars per face).

6.0 CONCLUSIONS

1. Iron-based shape memory alloys provide efficient and convenient means for rapid repair and strengthening of damaged or deficient elements of infrastructure. Restraint of shape recovery in these alloys can transfer corrective (post-tensioning) forces to structural systems. The process involves pre-elongation shape memory rods at ambient temperature, anchorage of pre-elongated rods onto the structural system, and electrical resistance heating (using a common generator) of rods to cause shape recovery and thus apply corrective forces to the structure.

2. Application of corrective forces by shape memory rods is a versatile approach capable of tackling diverse structural repair and strengthening problems. Laboratory and field tests verified the approach in applications involving repair of flexural and shear damages in reinforced concrete beams.

3. Recoverable strains of shape memory rods, when compared with elastic strains of steel and composites, are relatively large. Post-tensioning with shape memory rods is thus less prone to major losses of the prestressing force due to such factors as anchorage slippage and elastic shortening of structural elements.

4. Basic principles of prestressed concrete design can be adapted to develop design methodologies for repair and strengthening of structural systems with shape memory alloys.

5. Installed shape memory rods can re-apply corrective forces to structural systems (by electrical resistance heating) in case further damaging effects occur after installation of shape memory rods.

6. Application of corrective forces with shape memory alloys is an effective means of enhancing structural performance in diverse fields of applications. This approach could be used to control stresses, deflections or instabilities of diverse structural systems.

7.0 REFERENCES

1. Wayman, C.M. and Duerig, T.W., "An Introduction to Martensite and Shape Memory," Engineering Aspects of Shape Memory Alloys (T.W. Duerig, K.N. Melton, D. Stockel and C.M. Wayman, editors), Butterworth-Heinmann, Boston, 1990, pp. 3-21.
2. Otsuka, K. and Shimizu, K., "Pseudoelasticity and Shape Memory Effects in Alloys," International Metals Reviews, Vol. 31, No. 3, 1986, pp. 93-114.
3. Otsuka, H., "Fe-Mn-Si Based Shape Memory Alloys," Material Research Society Symposium Proceedings, Vol. 246, 1992, pp. 309-320.
4. Morriya, Y., Suzuki, H., Hashizume, S., Sampei, T. and Kozasu, I., "Effect of Alloying Element on Shape Memory Effect of Fe-Cr-Ni-Mn-Si Alloys," Proceedings, International Conference on Stainless Steels, 1991, pp. 527-532.
5. Murakami, M., Otsuka, H., Suzuki, H.G. and Matsuda, S., "Complete Shape Memory Effect n Polycrystalline Fe-Mn-Si Alloys," Proceedings, The International Conference on Martensitic Transformations, 1986, pp. 585-590.
6. Otsuka, H., Yamada, H., Tanahashi, H. and Maruyama, T., "Shape Memory Effect in Fe-Mn-Si-Cr-Ni Polycrystalline Alloys," Materials Science Forum, Vol. 56-58, 1990, pp. 655-660.
7. Nawy, E.G., "Prestressed Concrete," Prentice-Hall, 1996, 789 pp.

ACKNOWLEDGMENTS

Mr. Roger Till (Engineer of Structural Research, Michigan DOT) was instrumental in guiding the analytical and field efforts related to this project. Mr. Charles Arnold (formerly with Michigan DOT) played a key role in initiating the project, and continued to support the project throughout its implementation. Chris Idusuyi (Michigan DOT) and Jim Peterson (HNTB) also contributed towards implementation of the project.